JOURNAL OF GEOPHYSICAL RESEARCH: SPACE PHYSICS, VOL. 118, 6457–6464, doi:10.1002/jgra.50602, 2013

Cyclic reformation of a quasi-parallel bow shock at Mercury: MESSENGER observations

Torbjörn Sundberg,[1,2,3] Scott A. Boardsen,[2,4] James A. Slavin,[5] Vadim M. Uritsky,[2,6] Brian J. Anderson,[7] Haje Korth,[7] Daniel J. Gershman,[5] Jim M. Raines,[5] Thomas H. Zurbuchen,[5] and Sean C. Solomon[8,9]

Received 16 February 2013; revised 26 September 2013; accepted 26 September 2013; published 25 October 2013.

[1] We here document with magnetic field observations a passage of the MErcury Surface, Space ENvironment, GEochemistry, and Ranging (MESSENGER) spacecraft through Mercury's magnetosphere under conditions of a quasi-parallel bow shock, i.e., when the direction of the upstream interplanetary magnetic field was within 45° of the bow shock normal. The spacecraft's fast transition of the magnetosheath and the steady solar wind conditions during the period analyzed allow both spatial and temporal properties of the shock crossing to be investigated. The observations show that the shock reformation process can be nearly periodic under stable solar wind conditions. Throughout the 25-min-long observation period, the pulsation duration deviated by at most ~10% from the average 10 s period measured. This quasiperiodicity allows us to study all aspects of the shock reconfiguration, including ultra-low-frequency waves in the upstream region and large-amplitude magnetic structures observed in the vicinity of the magnetosheath-solar wind transition region and inside the magnetosheath. We also show that bow shock reformation can be a substantial source of wave activity in the magnetosphere, on this occasion having given rise to oscillations in the magnetic field with peak-to-peak amplitudes of 40–50 nT over large parts of the dayside magnetosphere. The clean and cyclic behavior observed throughout the magnetosphere, the magnetosheath, and the upstream region indicates that the subsolar region was primarily influenced by a cyclic reformation of the shock front, rather than by a spatial and temporal patchwork of short large-amplitude magnetic structures, as is generally the case at the terrestrial bow shock under quasi-parallel conditions.

Citation: Sundberg, T., S. A. Boardsen, J. A. Slavin, V. M. Uritsky, B. J. Anderson, H. Korth, D. J. Gershman, J. M. Raines, T. H. Zurbuchen, and S. C. Solomon (2013), Cyclic reformation of a quasi-parallel bow shock at Mercury: MESSENGER observations, *J. Geophys. Res. Space Physics*, *118*, 6457–6464, doi:10.1002/jgra.50602.

1. Introduction

[2] Shock fronts are abundant in space plasmas and are present both inherently in the solar wind and as bow shocks sunward of planets and comets, with the terrestrial bow shock the nearest and best-studied such object. These shock fronts serve important roles as they slow and thermalize the supersonic and super-Alfvénic plasma in the solar wind. Their behavior is highly dependent on the angle between the shock normal and the upstream magnetic field, θ_{BN}, and shocks are typically divided into quasi-parallel or quasi-perpendicular subsets, for which $\theta_{BN} < 45°$ and $\theta_{BN} > 45°$, respectively.

[3] Although the general properties of quasi-perpendicular shocks have been relatively well understood for decades, some questions regarding their internal spatial scales and their motion are still under investigation [e.g., *Paschmann et al.*, 1982; *Sckopke et al.*, 1990; *Bale et al.*, 2005]. In contrast, a full understanding of quasi-parallel shocks has not yet been reached, because of the highly intermittent nature of the quasi-parallel configuration and the resulting continuing process of reformation of the shock front, rendering the separation of spatial and temporal features difficult from single-spacecraft data. Multi-spacecraft crossings of the terrestrial shock region under quasi-parallel conditions have been key to advances in

[1]Center for Space Physics, Boston University, Boston, Massachusetts, USA.
[2]Heliophysics Science Division, NASA Goddard Space Flight Center, Greenbelt, Maryland, USA.
[3]School of Physics and Astronomy, Queen Mary University of London, London, UK.

Corresponding author: T. Sundberg, School of Physics and Astronomy, Queen Mary University of London, London E1 4NS, UK. (torbjorn.sundberg@gmail.com)

2169-9380/13/10.1002/jgra.50602

[4]Goddard Earth Sciences and Technology Center, University of Maryland, College Park, Maryland, USA.
[5]Department of Atmospheric, Oceanic and Space Sciences, University of Michigan, Ann Arbor, Michigan, USA.
[6]Catholic University of America, Washington, D.C., USA.
[7]The Johns Hopkins University Applied Physics Laboratory, Laurel, Maryland, USA.
[8]Lamont-Doherty Earth Observatory, Columbia University, Palisades, New York, USA.
[9]Department of Terrestrial Magnetism, Carnegie Institution of Washington, Washington, D.C., USA.

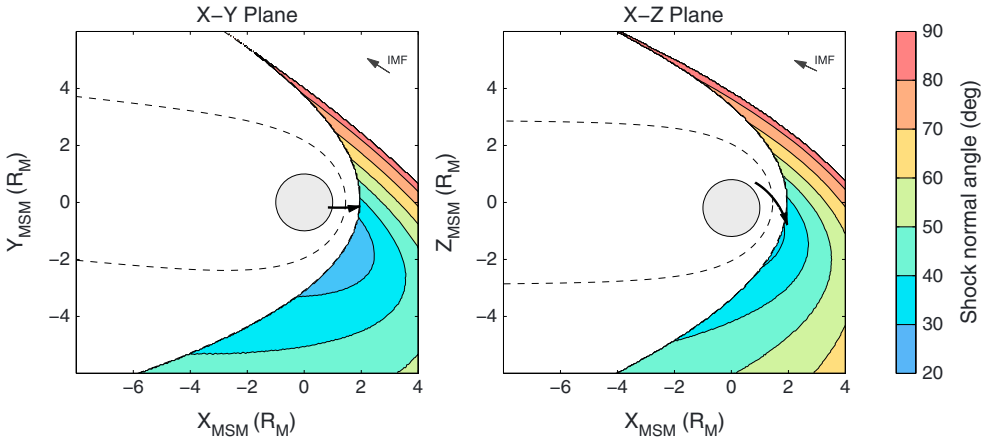

Figure 1. Projections of MESSENGER's trajectory onto the MSM *X–Y* (left) and *X–Z* (right) planes. The dashed lines show the average positions of the magnetopause and bow shock from the functional fit by *Winslow et al*. [2013], taking into account a 6° aberration of the solar wind flow direction. The shaded areas represent the upstream region of the solar wind magnetically connected to the bow shock, with the color coding indicating the IMF shock-normal angle. The thick arrow in the center of the plot represents MESSENGER's trajectory for the time period of interest, and the thin arrow in the top right corner shows the projection of the measured IMF direction onto each plane.

understanding [e.g., *Schwartz et al*., 1992; *Lucek et al*., 2002, 2008; *Behlke et al*., 2003, 2004; *Lefebvre et al*., 2009], as have computer simulations [e.g., *Burgess*, 1989; *Winske et al*., 1990; *Tsubouchi and Lembège*, 2004]. Together, observations and models have yielded a standard model for shock dynamics that includes all the components typically observed in association with quasi-parallel shocks: ion beams reflected at the shock front, upstream ultra-low-frequency (ULF) waves, short large-amplitude magnetic structures (SLAMS), and cyclic shock reconfiguration [e.g., *Burgess et al*., 2005].

[4] As the solar wind encounters the enhanced magnetic field at an undisturbed shock, the protons are accelerated and reflected upstream along the interplanetary magnetic field (IMF), forming high-velocity, sunward-propagating ion beams. These ion beams destabilize the plasma by the two-stream instability, leading to the generation of ULF waves in the upstream region. Although these ULF waves propagate sunward in the plasma frame of reference, they still convect toward the bow shock because of the high flow velocity of the solar wind. As they encounter suprathermal ions from the bow shock, the pulsations grow rapidly in amplitude, eventually forming into the SLAMS observed at Earth [e.g., *Giacalone et al*., 1993]. Each of these magnetic structures functions as a partial replacement of the original shock front, leading to the cyclic reformation process, as well as the possible injection of unshocked solar wind plasma into the magnetosheath. However, multi-spacecraft observations of bow shocks under quasi-parallel conditions are limited, and several aspects of the phenomena still remain to be determined, such as the spatial structure of SLAMS, their temporal evolution, and their growth rates [*Lucek et al*., 2008].

[5] Because of the low value of plasma β (the ratio of thermal to magnetic pressure) in the inner solar system, Mercury's bow shock is in general very weak compared with those at all other planets in our solar system [*Slavin and Holzer*, 1981], with sonic and Alfvénic Mach numbers of around 4–6. This weakness generally implies less particle heating at the shock, as well as smaller overshoots and shock ramps [*Masters et al*., 2013].

[6] We here document a crossing of Mercury's bow shock by the MErcury Surface, Space ENvironment, GEochemistry, and Ranging (MESSENGER) spacecraft during magnetic field conditions that exhibit many of the aspects attributed to quasi-parallel shocks at Earth. Although we do not have access to multipoint measurements, the small spatial scale of Mercury's magnetosphere together with the relatively high velocity of the spacecraft provides information on the spatial characteristics of quasiperiodic events for periods when solar wind conditions remain steady, during which the shock front exhibits a simple quasiperiodic temporal variation. This behavior allows us to investigate and link the processes in different regions, as well as to assess the impact of shock dynamics on Mercury's magnetosphere.

2. Observations

[7] The event selected and analyzed in this study took place on 11 August 2012, between 15:36 and 16:00 UTC, during a time when the bow shock was nearly periodic, as described below. During that period, the MESSENGER spacecraft traveled outward and southward though the northern hemisphere of the magnetosphere, crossed through the subsolar magnetosheath, and finally entered the solar wind, as shown in Figure 1. The projection of the trajectory onto Mercury's magnetic equatorial plane (Figure 1a) was nearly along the Mercury-Sun line.

[8] Magnetic field data for that interval collected by the MESSENGER Magnetometer instrument [*Anderson et al*., 2007] are shown in Figure 2. The data are here given in the Mercury solar magnetospheric (MSM) coordinate system, which is fixed at the center of the dipole component of Mercury's internal magnetic field, offset ~0.2 R_M (where R_M is Mercury's radius or 2440 km) northward of the planetary center [*Anderson et al*., 2011]. In the MSM system, the Cartesian (*X*, *Y*, *Z*) components are as follows: *Z* is positive

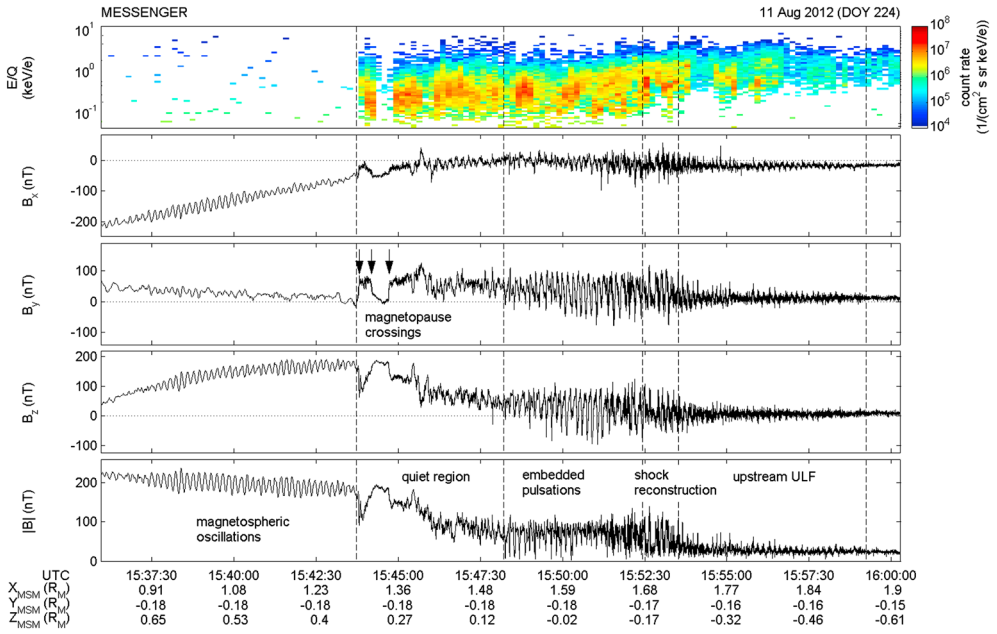

Figure 2. MESSENGER magnetic field measurements on 11 August 2012, showing strong wave activity in the (left) magnetosphere, (middle) the magnetosheath, and (right) the upstream solar wind. (top to bottom) The FIPS energy per charge spectrogram, the *X*, *Y*, and *Z* components of the magnetic field, and the magnetic field magnitude *B*. Three magnetopause crossings observed in the quiet region are marked by black arrows in the middle panel.

along the dipole axis, *X* is positive toward the Sun, and *Y* completes the right-hand system, positive duskward.

[9] As MESSENGER passed through the dayside magnetosphere, coherent sinusoidal oscillations in the magnetic field were seen (Figure 2). After the magnetopause crossing, there was a relatively quiet interval in the magnetosheath, but 4 min later (starting at ~15:48 UTC), the magnetosheath magnetic field experienced extreme pulsations during which the field magnitude periodically dropped from an average level of 80 nT to values of ~5–10 nT. Farther outward, these structures became increasingly intermittent, partly resembling the typical signature of SLAMS observed at quasi-parallel bow shocks at Earth [e.g., *Schwartz and Burgess*, 1991] and eventually diminished in amplitude until only a low-amplitude ULF wave pattern remained. The IMF was in a predominantly radial orientation ($B_X \approx -17$ nT, $B_Y \approx 11$ nT, $B_Z \approx 8$ nT) and relatively stable. A coplanarity analysis [e.g., *Abraham-Shrauner*, 1972] across this interval (15:51:30–15:55:00 UTC) suggests that $\theta_{BN} \approx 25°$ well within the limits of a quasi-parallel configuration. These calculations also agree well with the estimates of the angle between the IMF direction and shock normal in the foreshock region shown in Figure 1.

[10] The dominant pulsation period remained near ~10 s throughout the event, and the pulsations were extremely coherent, indicating both that there was a close relation between the upstream ULF waves and the magnetospheric oscillations and that the IMF likely remained steady throughout the interval. This period is approximately a factor of 3 greater than the ion cyclotron period in the undisturbed solar wind (~3 s).

[11] Wave properties for the wave structures measured in the frequency range 0.02–0.2 Hz, shown in Figure 3, highlight the change in wave characteristics across the interval. We discuss each region marked in Figures 2 and 3 in more detail in the subsections below, moving inward from the ULF growth region to the magnetosphere, because an examination in such a sequence best highlights the cause-and-effect relationship of the oscillations. The analysis will here focus primarily on the magnetic field observations, with some supporting data from MESSENGER's Fast Imaging Plasma Spectrometer (FIPS) [*Andrews et al.*, 2007] shown in Figure 2 (top).

[12] FIPS measures ions in an energy-per-charge range of 0.05–13 keV/e with an 8 s sampling time [*Raines et al.*, 2011]. The ion count rates are useful to identify long-term changes and characteristics of the ion population, but because the sampling period of the instrument is on the order of the dominant pulsation period of the event, the ion data do not resolve short-term variations in the plasma composition associated with the magnetic structures. The derivation of plasma moments from the instrument is also a non-trivial problem due to the restricted field of view of the instrument, and reliable particle densities and temperatures cannot readily be derived except under favorable conditions [*Raines et al.*, 2011]. On this occasion, FIPS was primarily measuring particles traveling southward and duskward. The instrument field of view is also partly obscured by the spacecraft sunshade, which prevents direct observations of the solar wind flow, and because of the near-radial direction of the IMF at the time, the instrument was not well oriented to observe field-aligned particle beams on this occasion; see *Gershman et al.* [2012] for details. This observing limitation also prevents us from making reliable estimates of the shock Mach number for this time period.

2.1. ULF Growth Region

[13] The low-amplitude ULF pulsations, shown in detail in Figure 4, were observed far upstream in the solar wind during this passage. The last wave oscillations were recorded at an

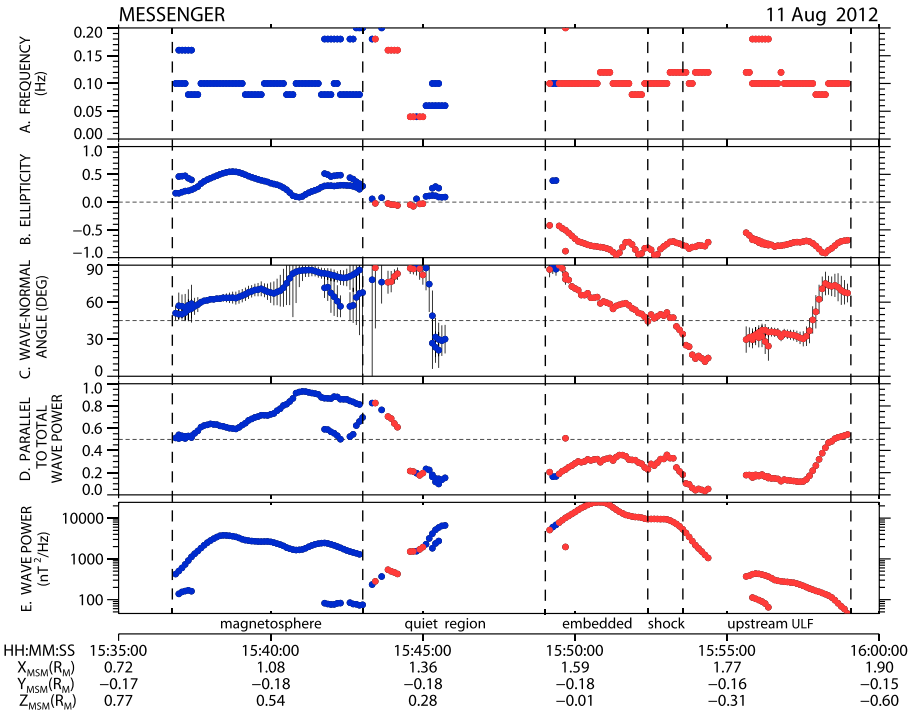

Figure 3. Overview of wave characteristics. (top to bottom) The dominant wave frequency, ellipticity, estimated wave-normal angles, ratio of the parallel to total wave power, and total wave power of the oscillations versus time and position in MSM coordinates. Each dot represents local maxima in wave power within the frequency span analyzed (0.02–0.2 Hz) with a total wave power exceeding 0.02 nT^2/Hz and the degree of polarization exceeding 0.8. Right-hand and left-hand polarized waves are represented by blue and red dots, respectively, and the vertical lines in Figure 3c show the standard deviation. The frequency resolution is 0.02 Hz, and each point covers an analysis period of 50 s. The white-noise coherency level is 0.40 with a standard deviation of 0.15 for the averaging used to compute the degree of polarization. A degree of polarization larger than 0.8 is thus 2.5 standard deviations above the noise level.

approximate spacecraft location of $X_{MSM} = 1.85$, $Y_{MSM} = 0.15$ R_M, and $Z_{MSM} = -0.5$ R_M, i.e., 0.5 R_M sunward of the outermost bow shock crossing, still close to the Sun-Mercury line and magnetically connected to the quasi-parallel bow shock. This limit may thus represent the outermost reach of the ULF disturbances at that time. As seen in Figure 3, the observations show waves with a 10 s recurrence period (Figure 3a) polarized in a left-handed sense (Figure 3b) and with low wave-normal angles (Figure 3c), similar to what was reported by *Fairfield and Behannon* [1976] from Mariner 10 observations near Mercury. Following the model of *Schwartz and Burgess* [1991], we interpret these oscillations as waves propagating upstream (sunward) in the plasma rest frame that were driven by the energetic ion beams reflected at the shock. However, as the bulk plasma convects with the solar wind velocity, the resultant wave motion is still expected to be directed toward the bow shock. This motion will lead to a polarization reversal in the spacecraft frame of reference, meaning that the left-handed polarization measured is actually the signature of right-handed mode waves.

[14] The interaction between the ion beams and the ULF waves leads to an increase in the wave power near the bow shock [e.g., *Burgess*, 1989; *Winske et al.*, 1990; *Dubouloz and Scholer*, 1993], as can be observed over the interval shown. In addition to the ULF waves, there was also a 2 Hz component present during this interval. These higher-frequency waves appear to be modulated by the ULF phase, with strong wave activity near the peaks of the low-frequency waves and low activity in between. Similar to the lower frequency waves, these 2 Hz waves were left-hand polarized in the spacecraft frame and had relatively circular polarization and low wave-normal angles. These waves were likely the same type as the whistler mode waves observed at Earth's bow shock, i.e., the so-called 1 Hz waves [e.g., *Orlowski et al.*, 1990; *Krauss-Varban et al.*, 1995; *Le et al.*, 2013].

[15] Ion measurements in the upstream region also reveal a plasma that is atypical for the solar wind, with a more diffuse distribution in energy than the typical case reported by *Gershman et al.* [2012] but similar to that expected in the foreshock. These particular observations do not allow for a reliable determination of the solar wind temperature or velocity separate from the upstream particle populations due to limitations in the sensor field of view. However, these data signal that we are not measuring cold particles that are flowing strictly sunward or antisunward but rather a population of hot particles associated with the shock reformation.

2.2. Shock Reformation

[16] An extract from the shock reformation region is shown in Figure 5. Isolated ~100 nT excursions from the ~20 nT IMF background are evident on the left side of the plot; in many ways these excursions are similar to those expected for SLAMS. The excursions are primarily in the B_Z and B_Y components of the magnetic field, i.e., mainly perpendicular to the

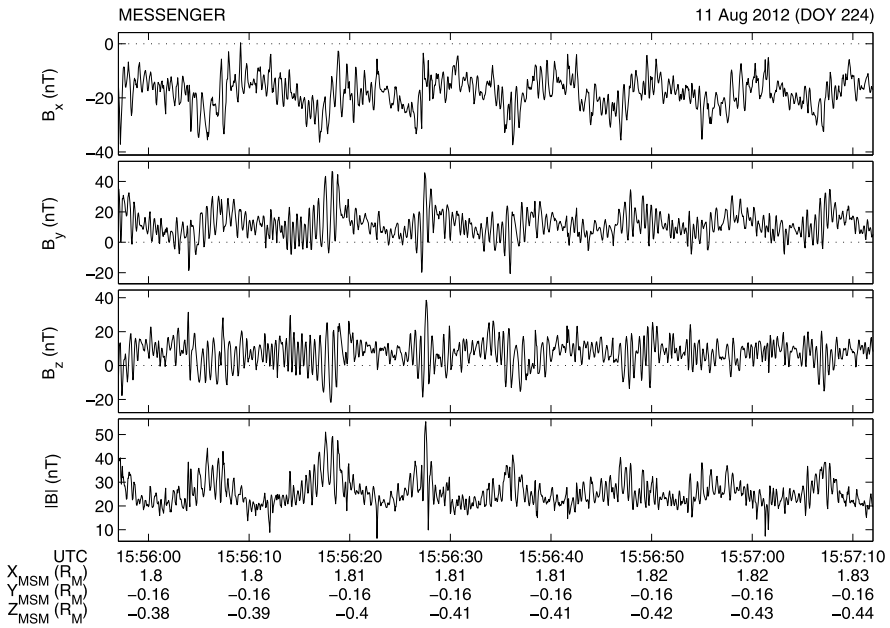

Figure 4. A close-up from the ULF wave growth region, showing both the 10 s oscillation of the ULF waves as well as the superposed 2 Hz waves, which are amplitude modulated by the ULF wave. This modulation is most clearly seen near 15:56:18 and 15:56:28 UTC.

background field. The measured left-hand polarization indicates a right-hand polarization in the wave reference frame, a result opposite to that which is generally reported at Earth, and each structure also shows a steepening at the planetward edge, contrary to that for terrestrial SLAMS for which the steepening is observed on the upstream (sunward) side [e.g., *Schwartz*, 1991; *Schwartz et al*., 1992]. There is also a high level of wave activity near ~2 Hz frequency at the upstream front, whereas the downstream transition is relatively undisturbed. These waves do not have a clear polarization in the shock reformation region, but they are similar to the upstream whistler waves in their frequency and burst characteristics, and they transition into a left-hand polarization upstream of the transition region.

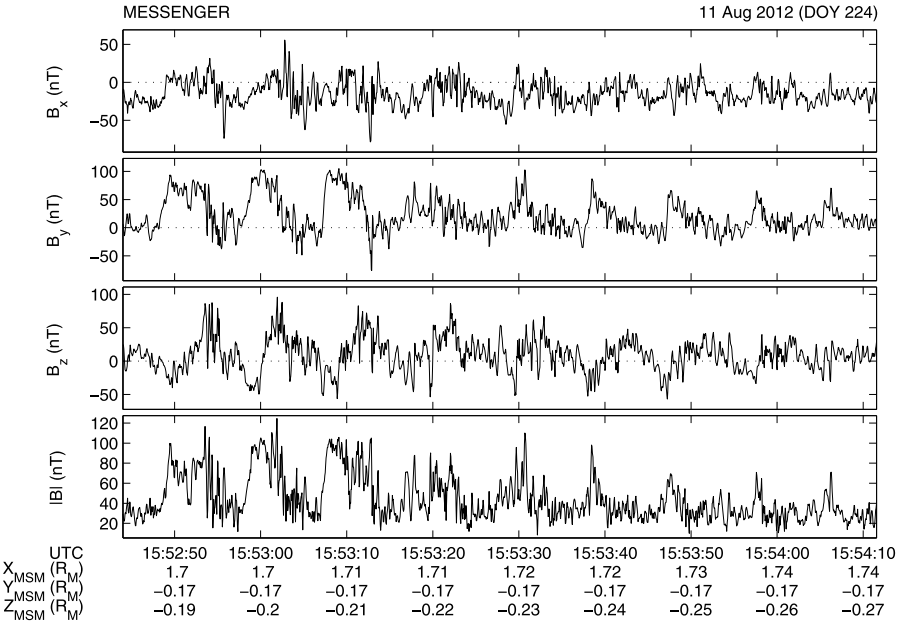

Figure 5. Close-up of the shock reformation region. Low-amplitude ULF waves are observed on the right, and large-amplitude magnetic structures due to bow shock reformation are seen on the left. A gradual change in amplitude can be observed over five wave periods between 15:53:10 and 15:53:50 UTC, indicating a clear connection between the two phenomena. A steepening can be observed on the left (downstream) side of both the fully developed and the intermediate-amplitude structures; a result opposite to that normally observed at the terrestrial bow shock.

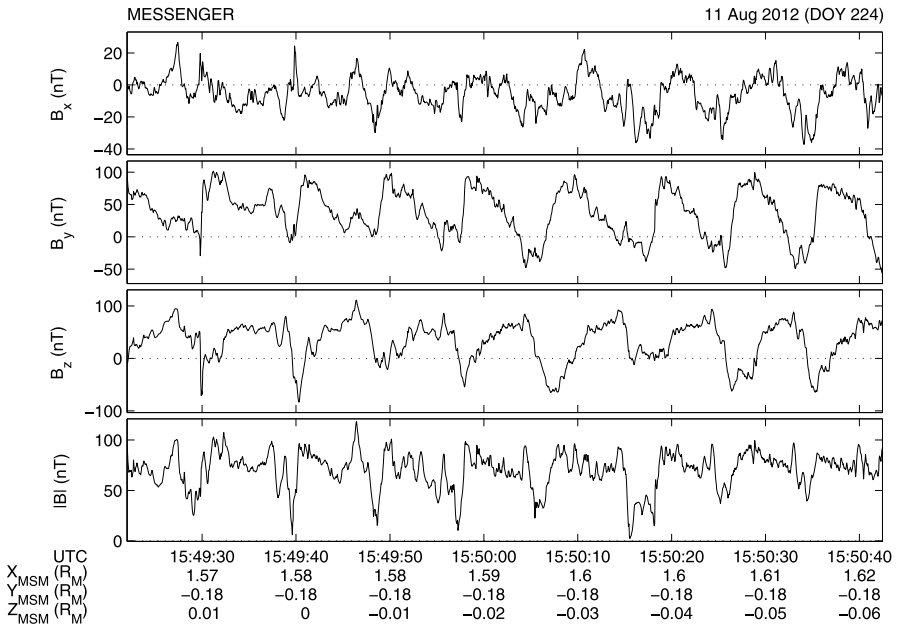

Figure 6. Close-up of observations in the magnetosheath showing the embedded pulsations, separated by short, 1–2 s long wake regions in which the magnetic field magnitude frequently drops to levels below 10 nT.

[17] The overall characteristics of the magnetosheath pulsations are illustrated in Figure 6. The structures shown are also left-hand polarized, with amplitudes of ~50 nT and a nearly constant field magnitude of ~80 nT, giving a relative wave amplitude $\Delta B/B$ of 0.6. Whereas the properties here were similar to those seen for the outer structures, the wake regions were substantially shorter, only 1–2 s, yet the field magnitude frequently dropped to values below 5 nT. These structures share some similarities with the embedded SLAMS reported by *Schwartz et al.* [1992], but they are of a more extreme character, and they are likely intimately connected with pressure fronts, as shown by *Giacalone et al.* [1993].

[18] The pulsations reached a maximum in wave power around 15:51 UTC, well within the magnetosheath (Figure 3e). They then slowly reduced in power toward the inner edge of the region at the same time that the wave-normal angle increased toward 90°. At the very end of the interval studied, these properties matched what may be expected for mirror mode waves [e.g., *Hasegawa*, 1969; *Herčík et al.*, 2013]. Such structures may thus be maintained by the mirror mode instability, but their initial source is more likely the bow shock reformation process.

2.3. Quiet Region

[19] The innermost part of the magnetosheath was relatively quiet during the passage described here, without any strong oscillations or magnetic depressions. Three consecutive magnetopause crossings were observed at 15:43:46, 15:44:10, and 15:44:42 UTC, each marked by a step-like change in the B_Y component and in the ion count rate, indicated by arrows in Figure 2. These multiple crossings were likely the result of an expansion-contraction or "breathing" motion of the magnetopause. The magnetosheath magnetic field was strongest near the magnetopause and decreased gradually as MESSENGER traveled outward from the magnetosphere.

[20] There are two possible explanations for the absence of waves and wake regions in the magnetosheath. First, the wave motion may be damped deep in the magnetosheath so that the magnetic field stabilizes at a relatively constant level irrespective of the pressure oscillations associated with the embedded pulsations farther sunward. Alternatively, because of its location substantially northward of the ecliptic plane, the spacecraft may have been outside of the main shock reformation region, which, given the IMF orientation ($B_X < 0$ and $B_Z > 0$), should have been biased toward the southern hemisphere. Given the sudden drop in wave power and that the pressure pulses still penetrated within the magnetosphere, we believe that the second explanation provides a better match to the data.

2.4. Magnetospheric Pulsations

[21] Pulsations in the planetary magnetic field were present between 15:36 and 15:43 UTC (the innermost magnetopause crossing). These temporal boundaries are equivalent to L shells of approximately 1.35 and 1.4, respectively, where the L value represents the field line's radius in the equatorial plane, given in units of R_M [*McIlwain*, 1961]. The waves were linearly polarized along the magnetic field direction (i.e., purely compressional) near the magnetopause, as can be seen in the high ratio of field-parallel power to total wave power in Figure 3d. This polarization then gradually changed deeper into the magnetosphere, with the innermost oscillations showing right-hand polarization and wave-normal angles of ~60°. The pulsation period remained extremely stable at 10 s throughout the transit, and the peak-to-peak wave amplitude was steady at ~40–50 nT.

3. Discussion

[22] The main pulsation period was extremely stable throughout the entire event, varying only by ~10%, with close to identical frequencies observed in the solar wind, the magnetosheath, and the magnetosphere, as shown in Figure 3. This steady behavior indicates both that IMF

conditions were relatively stable throughout the event and that there was a clear interaction between the bow shock and the magnetosphere on this occasion. The magnetospheric waves may likely have been driven by pressure fronts connected to the shock reformation. Although we do not know the details of the plasma distribution in the magnetosheath, either in the peak or the wake regions, the change in magnetic pressure, $B^2/2\mu_0$ (where μ_0 is the permeability of free space), resulting from the observed 10–80 nT cycles equals 2.5 nPa. This change is comparable to an increase in the subsolar magnetopause field from 160 to nearly 180 nT, which accounts for about half the amplitude of the magnetospheric wave pattern observed.

[23] From terrestrial observations, SLAMS and wake regions are also known to be correlated with density and temperature variations, with the SLAMS dense and non-thermalized and the inter-SLAMS regions rarified and heated by the reflected solar wind ions [*Thomsen et al*., 1990; *Schwartz et al*., 1992], a relation that may add to the pressure imbalance. The observations at Mercury documented here could thus be the result of propagating pressure pulses that periodically compress and relax the magnetosphere, leading to the compressional waves observed near the subsolar magnetopause that then couple to the elliptical waves observed deeper within the magnetosphere. The quasi-parallel bow shock may thus be a direct source of energy input into the magnetosphere, although electric field measurements would be necessary to establish the Poynting flux and evaluate the total energy input. These magnetospheric oscillations are similar to those observed in connection with Kelvin-Helmholtz waves at the magnetopause [*Sundberg et al*., 2012] and should be considered as another possible source of the ~0.1 Hz quasi-oscillations frequently seen throughout Mercury's magnetosphere. We also note that the concept of bow shock-magnetosphere coupling has previously been observed at Earth, where multi-spacecraft observations have linked pulsations inside the magnetosphere and the magnetosheath to upstream pressure variations associated with the bow shock [*Fairfield et al*., 1990; *Archer et al*., 2012; *Archer and Horbury*, 2013].

[24] Thanks to the quasi-steady behavior of the oscillations, the observations permit an approximate estimate of the length scale of the growth region of the magnetic structures. A clear trend is seen in Figure 5, with a gradual transition from ULF waves on the right to fully developed structures on the left over 5–6 pulsation cycles, during which MESSENGER traveled approximately 0.06 R_M, or 140–150 km. Of course, the "quasi-steady" assumption invoked here warrants caution, and further studies are needed to constrain these values well. To put these figures in context, they can be compared with an average thickness of the subsolar magnetosheath of ~0.5 R_M [*Winslow et al*., 2013] or an upstream ion cyclotron radius of ~50 km for a 100 eV proton. The gyroradius of a solar wind ion at the shock front is likewise estimated to be ~50 km for a solar wind velocity of 400 km/s and a downstream magnetic field of 80 nT. It should also be noted that partly steepened, large-amplitude ULF pulsations are sometimes observed farther from the bow shock region. The last steepened structure was recorded at about 15:55:50 UTC with a short peak at 70 nT, approximately 0.15 R_M (360–370 km) from the fully developed structures in Figure 5.

[25] Since the magnetospheric pulsations are clear and quasiperiodic, each oscillation is likely to be the direct effect of a pressure impulse from a single-shock reconfiguration front, similar to what was reported by *Lefebvre et al*. [2009], rather than the result of a spatially distributed patchwork of SLAMS as is the general picture given for the terrestrial magnetosphere under quasi-parallel shock conditions. By this inference, the spatial cross section of the observed structures must be relatively large in order to establish a dominant periodicity in the dayside region, likely around ~2 R_M, as we otherwise would have expected a more disturbed oscillation within the magnetosphere, driven by a series of phase-shifted SLAMS at different locations along the magnetopause. Because the IMF direction deviates from the solar wind direction in this case, there should also be a spatial separation between the point of origin of the reflected ions at the bow shock and the eventual impact point of the resulting structure, possibly up to 0.25 R_M on the basis of an extent of the ULF region of 0.5 R_M and an angle between the IMF and the solar wind velocity of ~30° (taking into account solar wind aberration). If the cross-sectional scale of individual structures were relatively short (i.e., there were a patchwork of SLAMS), we would also have expected a less stable period in the ULF wave field as the upstream region would have been disturbed by neighboring SLAMS, causing variations in the SLAMS recurrence period.

4. Conclusions

[26] The overall characteristics of the bow shock crossing at Mercury examined in this paper are in good agreement with the models developed from quasi-parallel bow shock crossings at Earth [e.g., *Schwartz and Burgess*, 1991; *Burgess et al*., 2005]. Such models provide an explanation for how upstream ULF pulsations grow into solitary and embedded SLAMS and inject wake regions with low magnetic fields into the magnetosheath. However, the structures observed here differ from those of terrestrial SLAMS in their polarization, as the observations indicate a right-handed rotation compared with generally left-hand polarized SLAMS at Earth. These conclusions are predicated on the assumption that the structures convect downstream with the solar wind flow. This assumption may be overly simplified, as the field-aligned motion of the reflected ions is not strictly sunward, which adds a component perpendicular to the Sun-aligned axis to the direction of motion of the shock front, but a scenario by which MESSENGER encountered the leading edge of the shock before the trailing edge seems unlikely. Unfortunately, as the field of view and time resolution of the FIPS measurements limit our knowledge of the ion population, the details of the propagation direction and velocity of the upstream ions are unknown, so we are prevented from investigating the details of the driving mechanisms that led to the shock reformation.

[27] In addition to illuminating the growth process of the structures observed through the magnetosheath and foreshock region, the observations also highlight several key issues on quasi-parallel bow shock crossings in general, and at small magnetospheres in particular, to an extent that has not previously been observed at Earth:

[28] 1. The stable frequency observed in the magnetosphere indicates that the subsolar magnetosphere was primarily influenced by a cyclic shock reconfiguration, rather than a patchwork of quasi-simultaneous SLAMS, as is the general case at the terrestrial bow shock.

[29] 2. There is an inherent reformation frequency attributed to the quasi-parallel bow shock, given stable solar wind conditions. For this event at Mercury, the reformation period was estimated to be ~3 times the ion gyroperiod in the undisturbed solar wind.

[30] 3. The bow shock can be a direct source of low-frequency wave energy in the outer magnetosphere by periodic cycling of the pressure applied at the magnetopause by the magnetosheath.

[31] 4. Although the pulsations observed here are similar to terrestrial SLAMS, the steepening is observed on the opposite side. We have yet to determine the cause of this difference and whether this result is a common or unusual phenomenon at Mercury's bow shock.

[32] **Acknowledgments.** The MESSENGER project is supported by the NASA Discovery Program under contracts NAS5-97271 to The Johns Hopkins University Applied Physics Laboratory and NASW-00002 to the Carnegie Institution of Washington. This research was also supported by the NASA Postdoctoral Program at the Goddard Space Flight Center, administered by Oak Ridge Associated Universities through a contract with NASA, and by the NASA Planetary Data Analysis Program grant NNX10AU26G.

[33] Masaki Fujimoto thanks the reviewers for their assistance in evaluating this paper.

References

Abraham-Shrauner, B. (1972), Determination of magnetohydrodynamic shock normals, *J. Geophys. Res.*, *77*, 736–739, doi:10.1029/JA077i004p00736.

Anderson, B. J., M. H. Acuña, D. A. Lohr, J. Scheifele, A. Raval, H. Korth, and J. A. Slavin (2007), The Magnetometer instrument on MESSENGER, *Space Sci. Rev.*, *131*, 417–450.

Anderson, B. J., C. L. Johnson, H. Korth, M. E. Purucker, R. M. Winslow, J. A. Slavin, S. C. Solomon, R. L. McNutt Jr., J. M. Raines, and T. H. Zurbuchen (2011), The global magnetic field of Mercury from MESSENGER orbital observations, *Science*, *333*, 1859–1862.

Andrews, G. B., et al. (2007), The Energetic Particle and Plasma Spectrometer instrument on the MESSENGER spacecraft, *Space Sci. Rev.*, *131*, 523–556.

Archer, M. O., and T. S. Horbury (2013), Magnetosheath dynamic pressure enhancements: Occurrence and typical properties, *Ann. Geophys.*, *31*, 319–331, doi:10.5194/angeo-31-319-2013.

Archer, M. O., T. S. Horbury, and J. P. Eastwood (2012), Magnetosheath pressure pulses: Generation downstream of the bow shock from solar wind discontinuities, *J. Geophys. Res.*, *117*, A05228, doi:10.1029/2011JA017468.

Bale, S. D., et al. (2005), Quasi-perpendicular shock structure and processes, *Space Sci. Rev.*, *118*, 161–203, doi:10.1007/s11214-005-3827-0.

Behlke, R., M. André, S. C. Buchert, A. Vaivads, A. I. Eriksson, E. A. Lucek, and A. Balogh (2003), Multi-point electric field measurements of short large-amplitude magnetic structures (SLAMS) at the Earth's quasi-parallel bow shock, *Geophys. Res. Lett.*, *30*(4), 1177, doi:10.1029/2002GL015871.

Behlke, R., M. André, S. D. Bale, J. S. Pickett, C. A. Cattell, E. A. Lucek, and A. Balogh (2004), Solitary structures associated with short large-amplitude magnetic structures (SLAMS) upstream of the Earth's quasi-parallel bow shock, *Geophys. Res. Lett.*, *31*, L16805, doi:10.1029/2004GL019524.

Burgess, D. (1989), Cyclic behavior at quasi-parallel collisionless shocks, *Geophys. Res. Lett.*, *16*, 345–348, doi:10.1029/GL016i005p00345.

Burgess, D., et al. (2005), Quasi-parallel shock structure and processes, *Space Sci. Rev.*, *118*, 205–222, doi:10.1007/s11214-005-3832-3.

Dubouloz, N., and M. Scholer (1993), On the origin of short large-amplitude magnetic structures upstream of quasi-parallel collisionless shocks, *Geophys. Res. Lett.*, *20*, 547–550, doi:10.1029/93GL00803.

Fairfield, D. H., and K. W. Behannon (1976), Bow shock and magnetosheath waves at Mercury, *J. Geophys. Res.*, *81*, 3897–3906, doi:10.1029/JA081i022p03897.

Fairfield, D. H., W. Baumjohann, G. Paschmann, H. Lühr, and D. G. Sibeck (1990), Upstream pressure variations associated with the bow shock and their effects on the magnetosphere, *J. Geophys. Res.*, *95*, 3773–3786, doi:10.1029/JA095iA04p03773.

Gershman, D. J., T. H. Zurbuchen, L. A. Fisk, J. A. Gilbert, J. M. Raines, B. J. Anderson, C. W. Smith, H. Korth, and S. C. Solomon (2012), Solar wind alpha particles and heavy ions in the inner heliosphere observed with MESSENGER, *J. Geophys. Res.*, *117*, A00M02, doi:10.1029/2012JA017829.

Giacalone, J., S. J. Schwartz, and D. Burgess (1993), Observations of suprathermal ions in association with SLAMS, *Geophys. Res. Lett.*, *20*, 149–152, doi:10.1029/93GL00067.

Hasegawa, A. (1969), Drift mirror instability in the magnetosphere, *Phys. Fluids*, *12*, 2642–2650, doi:10.1063/1.1692407.

Herčík, D., P. M. Trávníček, J. R. Johnson, E.-H. Kim, and P. Hellinger (2013), Mirror mode structures in the asymmetric Hermean magnetosheath: Hybrid simulations, *J. Geophys. Res. Space Physics*, *118*, 405–417, doi:10.1029/2012JA018083.

Krauss-Varban, D., F. G. E. Pantellini, and D. Burgess (1995), Electron dynamics and whistler waves at quasi-perpendicular shocks, *Geophys. Res. Lett.*, *22*, 2091–2094, doi:10.1029/95GL01782.

Le, G., P. J. Chi, X. Blanco-Cano, S. Boardsen, J. A. Slavin, and B. J. Anderson (2013), Upstream ultra-low frequency waves in Mercury's foreshock region: MESSENGER magnetic field observations, *J. Geophys. Res. Space Physics*, *118*, 2809–2823, doi:10.1002/jgra.50342.

Lefebvre, B., Y. Seki, S. J. Schwartz, C. Mazelle, and E. A. Lucek (2009), Reformation of an oblique shock observed by Cluster, *J. Geophys. Res.*, *114*, A11107, doi:10.1029/2009JA014268.

Lucek, E. A., T. S. Horbury, M. W. Dunlop, P. J. Cargill, S. J. Schwartz, A. Balogh, P. Brown, C. Carr, K.-H. Fornacon, and E. Georgescu (2002), Cluster magnetic field observations at a quasi-parallel bow shock, *Ann. Geophys.*, *20*, 1699–1710.

Lucek, E. A., T. S. Horbury, I. Dandouras, and H. Rème (2008), Cluster observations of the Earth's quasi-parallel bow shock, *J. Geophys. Res.*, *113*, A07S02, doi:10.1029/2007JA012756.

Masters, A., J. A. Slavin, G. A. DiBraccio, T. Sundberg, R. M. Winslow, C. L. Johnson, B. J. Anderson, and H. Korth (2013), A comparison of magnetic overshoots at the bow shocks of Mercury and Saturn, *J. Geophys. Res. Space Physics*, *118*, 4381–4390, doi:10.1002/jgra.50428.

McIlwain, C. E. (1961), Coordinates for mapping the distribution of magnetically trapped particles, *J. Geophys. Res.*, *66*, 3681–3691, doi:10.1029/JZ066i011p03681.

Orlowski, D. S., G. K. Crawford, and C. R. Russell (1990), Upstream waves at Mercury, Venus and Earth: Comparison of the properties of one Hertz waves, *Geophys. Res. Lett.*, *17*, 2293–2296, doi:10.1029/GL017i013p02293.

Paschmann, G., N. Sckopke, S. J. Bame, and J. T. Gosling (1982), Observations of gyrating ions in the foot of the nearly perpendicular bow shock, *Geophys. Res. Lett.*, *9*, 881–884, doi:10.1029/GL009i008p00881.

Raines, J. M., J. A. Slavin, T. H. Zurbuchen, G. Gloeckler, B. J. Anderson, D. N. Baker, H. Korth, S. M. Krimigis, and R. L. McNutt Jr. (2011), MESSENGER observations of the plasma environment near Mercury, *Planet. Space Sci.*, *59*, 2004–2015, doi:10.1016/j.pss.2011.02.004.

Schwartz, S. J. (1991), Magnetic field structures and related phenomena at quasi-parallel shocks, *Adv. Space Res.*, *11*, 231–240, doi:10.1016/0273-1177(91)90039-M.

Schwartz, S. J., and D. Burgess (1991), Quasi-parallel shocks: A patchwork of three-dimensional structures, *Geophys. Res. Lett.*, *18*, 373–376, doi:10.1029/91GL00138.

Schwartz, S. J., D. Burgess, W. P. Wilkinson, R. L. Kessel, M. Dunlop, and H. Lühr (1992), Observations of short large-amplitude magnetic structures at a quasi-parallel shock, *J. Geophys. Res.*, *97*, 4209–4227, doi:10.1029/91JA02581.

Sckopke, N., G. Paschmann, A. L. Brinca, C. W. Carlson, and H. Lühr (1990), Ion thermalization in quasi-perpendicular shocks involving reflected ions, *J. Geophys. Res.*, *95*, 6337–6352, doi:10.1029/JA095iA05p06337.

Slavin, J. A., and R. E. Holzer (1981), Solar wind flow about the terrestrial planets, 1. Modeling bow shock position and shape, *J. Geophys. Res.*, *86*, 11,401–11,418, doi:10.1029/JA086iA13p11401.

Sundberg, T., S. A. Boardsen, J. A. Slavin, B. J. Anderson, H. Korth, T. H. Zurbuchen, J. M. Raines, and S. C. Solomon (2012), MESSENGER orbital observations of large-amplitude Kelvin-Helmholtz waves at Mercury's magnetopause, *J. Geophys. Res.*, *117*, A04216, doi:10.1029/2011JA017268.

Thomsen, M. F., J. T. Gosling, S. J. Bame, T. G. Onsager, and C. T. Russell (1990), Two-state ion heating at quasi-parallel shocks, *J. Geophys. Res.*, *95*, 6363–6374, doi:10.1029/JA095iA05p06363.

Tsubouchi, K., and B. Lembège (2004), Full particle simulations of short large-amplitude magnetic structures (SLAMS) in quasi-parallel shocks, *J. Geophys. Res.*, *109*, A02114, doi:10.1029/2003JA010014.

Winske, D., N. Omidi, K. B. Quest, and V. A. Thomas (1990), Re-forming supercritical quasi-parallel shocks, 2. Mechanism for wave generation and front re-formation, *J. Geophys. Res.*, *95*, 18,821–18,832, doi:10.1029/JA095iA11p18821.

Winslow, R. M., B. J. Anderson, C. L. Johnson, J. A. Slavin, H. Korth, M. E. Purucker, D. N. Baker, and S. C. Solomon (2013), Mercury's magnetopause and bow shock from MESSENGER Magnetometer observations, *J. Geophys. Res. Space Physics*, *118*, 2213–2227, doi:10.1002/jgra.50237.